Date of publication xxxx 00, 0000, date of current version xxxx 00, 0000.

Digital Object Identifier 10.1109/ACCESS.2018.DOI

Weighted Incoherent Signal Subspace Method for DOA Estimation on Wideband Colored Signals

YECHAO BAI[1], JIANGHUI LI[2], YU WU[1], QIONG WANG[1], AND XINGGAN ZHANG[1]
[1]School of Electronic Science and Engineering, Nanjing University, Nanjing, 210023 China
[2]Institute of Sound and Vibration Research, University of Southampton, Southampton, S017 1BJ, UK

Corresponding author: Qiong Wang (e-mail: wangqiong@nju.edu.cn).

This work was supported in part by the National Natural Science Foundation of China under Grant 61571220, and in part by the Basic Research Program of Jiangsu Province under Grant BK20151391.

ABSTRACT Wideband direction-of-arrival (DOA) estimation is a key part in array signal processing. Existing algorithms for the wideband DOA estimation are often studied in the situation of uniformly distributed energy. And all the frequency bins are weighted equally in these algorithms. However, these algorithms perform unsatisfactorily when encountering wideband colored signals with nonuniform energy spectrum. To improve the performance of DOA estimation for wideband colored signals, we proposed two weighting methods, which are based on the perturbed subspace theory and random matrix theory respectively. The two methods weight the space spectrum from all the frequency bins according to the mean square error (MSE) of DOA estimation in each frequency bin. Numerical results show that the random matrix theory based method performs well, due to the inference premise that the dimensions of matrices increase at the same rate. The perturbed subspace based method, which is concise in calculating the weights, shows high accuracy only at high signal to noise ratio (SNR) and with adequate snapshots. The effectiveness of the two algorithms are also demonstrated by comparing them to various existing algorithms and the Cramér-Rao bound.

INDEX TERMS Direction-of-arrival estimation, random matrix theory, signal subspace method, wideband signal.

I. INTRODUCTION

ARRAYS have been widely used in radar and communication systems, and provide an invaluable tool in smart cities [1], [2]. In array signal processing, direction-of-arrival (DOA) estimation is an important part [3], [4]. The array signal model of narrowband sources can be simplified from the straightforward correlation between the DOA and the phase shift [5]–[7]. Methods for DOA estimation of narrowband sources have been presented in literatures, such as the maximum likelihood (ML) method [8], the multiple signal classification (MUSIC) algorithm [6], and the estimation of signal parameters via rotational invariance techniques (ESPRIT) [9].

However, DOA estimation of wideband sources has not been widely investigated. Different from narrowband sensor arrays, the phase shift between sensor outputs of wideband arrays not only relies on the DOA, but also on the temporal frequency, which varies in a large scope. Therefore, methods for narrowband DOA estimation cannot be applied to wideband circumstances directly.

One intuitive way for wideband DOA estimation is to decompose the wideband signal into a number of narrowband components, and then take advantage of the narrowband covariance matrices to obtain better estimation performance than using narrowband methods directly. One of such methods is known as coherent signal subspace method (CSSM), which transforms the narrowband covariance matrices from all the subbands into a single frequency via focusing matrices, and then the narrowband DOA estimation is performed on the focusing frequency [11]. Two general forms for calculating signal subspace transformation matrices have been presented [12]. These transformation matrices are well known for their optimality in terms of preserving signal to noise ratio (SNR) after focusing different frequencies. Another method known as weighted average of signal subspaces (WAVES) combines focusing matrices and the weighted subspace fit-

ting to improve the robustness of CSSM [13]. Initial DOA values are necessary to construct the focusing matrices in both CSSM and WAVES. The estimation accuracy of the two methods are sensitive to the initial values of DOA.

An interpolation technique, constructing a virtual array for each frequency to obtain the same array manifold [14], and the array manifold interpolation applied into two dimensional arrays with known arbitrary geometries [15] have been presented. For DOA estimation on wideband signals without preprocessing initial values, a test of orthogonality of projected subspaces (TOPS) method has been proposed [16]. The TOPS estimates DOAs by measuring the orthogonal relation between the signal and the noise subspaces of multiple frequency components of the sources. This method formulates a test in which the rank of a matrix decreases when the assumed angle in the test equals to one of the DOAs, and well performs in mid SNR ranges. The incoherent signal subspace method (ISSM) decomposes the wideband signal into narrowband components, and carries out the computation in each narrowband [17], [18]. ISSM requires no initial DOA value, whereas it suffers when the SNR at each frequency bin varies, because the DOA estimate at some frequencies may show poor performance [16].

The ML method can also be used for wideband DOA estimation. The relationship between ML of the deterministic model and ML of the Gaussian model in wideband DOA estimation has been examined in [19]. ESPRIT algorithm was extended from narrowband signals to wideband signals in [20]. Recent development of compressive sensing inspires researchers to study wideband DOA estimation from the view of sparse representation [21]–[23]. These sparse representation methods explore the sparsity of sources in the spatial space, and estimate DOAs by ℓ_1 norm minimisation.

Most of these methods for wideband DOA estimation assume that the SNRs of all frequency bins keep the same. While the SNR at different frequency bins usually vary because of the inherent nonuniform power spectrum of the wideband sources or the fluctuating amplitude-frequency characteristic of the sensors in array. This means that we need to handle wideband colored signals, where the power spectral density is not flat throughout the frequency spectrum. In this work, we calculate the weight for each frequency bin of wideband colored signals to improve the accuracy of the ISSM. The proposed algorithm performs well and does not need any initial value.

The rest of the paper is organized as follows. The studied problem is formulated in Section II. In Section III, we study the performance of DOA estimation for narrow band signals in a couple of different approaches, the perturbed subspace based approach and the random matrix theory based approach. The methods for weighting the space spectrum are proposed in Section IV. The numerical results based on Monte Carlo simulations are shown in Section V. Section VI completes the paper with concluding remarks.

II. PROBLEM FORMULATION

Consider Q wideband source signals from the far-field directions $\boldsymbol{\theta} = [\theta_1, ..., \theta_Q]^T$ impinging on a uniform linear array with N sensors, which are spaced d apart, where $(\cdot)^T$ denotes the transpose. Each sensor signal is time sampled and partitioned into M segments (frequency snapshots). K complex subband components are generated by applying the discrete Fourier transform (DFT) to each segment, such that each subband snapshot can be modeled as [23]

$$\mathbf{x}_m(f_k) = \mathbf{A}_k(\boldsymbol{\theta})\mathbf{s}_m(f_k) + \mathbf{n}_m(f_k),\ k \in [K],\ m \in [M], \tag{1}$$

where $\mathbf{x}_m(f_k) \in \mathbb{C}^N$, $\mathbf{s}_m(f_k) \in \mathbb{C}^Q$, $\mathbf{n}_m(f_k) \in \mathbb{C}^N$ are the DFT coefficients of the received data, source signals and additive noises, respectively, and $[K] \triangleq \{1, 2, ..., K\}$, $\mathbf{A}_k(\boldsymbol{\theta}) = [\mathbf{a}_k(\theta_1), ..., \mathbf{a}_k(\theta_Q)] \in \mathbb{C}^{N\times Q}$ is the steering matrix at the frequency bin f_k with steering vector

$$\mathbf{a}_k(\theta_q) = \left[1, e^{\frac{j2\pi f_k d\sin(\theta_q)}{c}}, ..., e^{\frac{j2\pi f_k (N-1) d\sin(\theta_q)}{c}}\right]^H, \tag{2}$$

where c is the propagation speed and $(\cdot)^H$ denotes the conjugate transpose.

Due to the power variation among frequency bins of the transmitted signal and the fluctuations of frequency responses for the array sensors, the power of each source signal may be distributed nonuniformly among frequency bins. This means the array may receive wideband colored signals. The additive noises within different frequency bins are assumed to be complex Gaussian distributed, and independent of each other [18], [23]. Consider the sensors have equal noise power within the same frequency bin. The variance of the noise within the kth frequency bin is denoted as σ_k^2. The received snapshot vectors within each frequency bin are stacked in a data matrix,

$$\mathbf{X}_k = [\mathbf{x}_1(f_k), ..., \mathbf{x}_M(f_k)] = \mathbf{A}_k(\boldsymbol{\theta})\mathbf{S}_k + \mathbf{N}_k, \tag{3}$$

where $\mathbf{S}_k = [\mathbf{s}_1(f_k), ..., \mathbf{s}_M(f_k)]$ is the matrix of the source signals, and $\mathbf{N}_k = [\mathbf{n}_1(f_k), ..., \mathbf{n}_M(f_k)]$ is the noise matrix .

Denote the singular value decomposition (SVD) of $\mathbf{X}_k$ as $\hat{\mathbf{U}}_k\hat{\mathbf{\Lambda}}_k\hat{\mathbf{V}}_k^H$, where $\hat{\mathbf{U}}_k = [\hat{\mathbf{u}}_k, \hat{\mathbf{U}}_k^{\perp}]$. The singular values of $\mathbf{X}_k$ are sorted decreasingly. $\hat{\mathbf{u}}_k$ is the left singular vector corresponding to the largest singular value and the corresponding right singular vector is $\hat{\mathbf{v}}_k$. $\hat{\mathbf{U}}_k^{\perp}$ consists of all the vectors in $\hat{\mathbf{U}}_k$ except $\hat{\mathbf{u}}_k$.

We first consider the situation with only one source signal from direction θ_1. Denote the signal of the kth frequency bin in the mth segment as $s_m(f_k)$. Equation (1) can be rewritten as

$$\mathbf{x}_m(f_k) = \sqrt{M\sigma_k^2}\left[\sqrt{SNR_k}\mathbf{u}_k(\theta_1)\frac{1}{\sqrt{ME_k}}s_m(f_k) + \frac{1}{\sqrt{M\sigma_k^2}}\mathbf{n}_m(f_k)\right],\ k \in [K],\ m \in [M], \tag{4}$$

where $E_k = \frac{1}{M}\sum_{m=1}^{M}|s_m(f_k)|^2$ is the average power of source signal at frequency f_k, $SNR_k = NE_k/\sigma_k^2$ is the

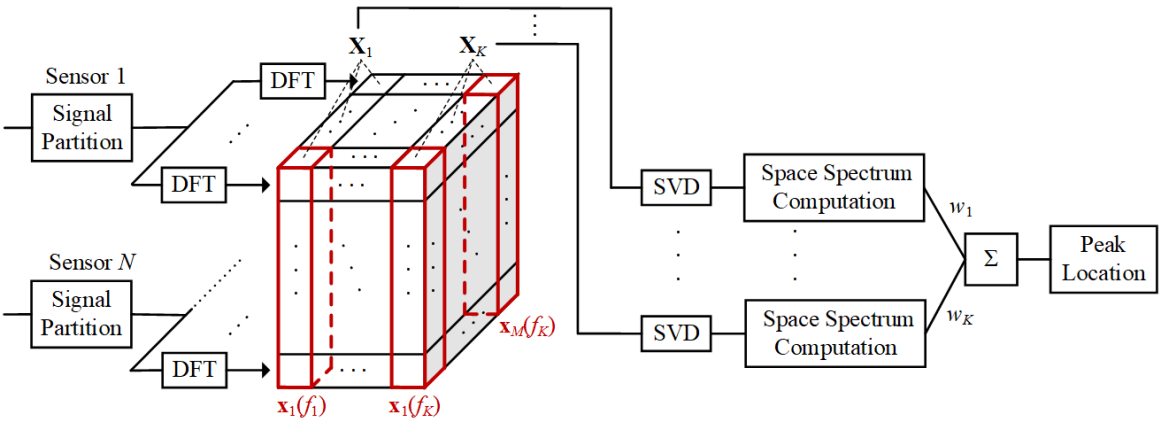

FIGURE 1. Block diagram of the weighted incoherent signal subspace method.

array SNR, and $\mathbf{u}_k(\theta_1) = \mathbf{a}_k(\theta_1)/\sqrt{N}$ is a unit-norm vector. Let $\mathbf{v}_k = [s_1(f_k), ..., s_M(f_k)]/\sqrt{ME_k}$. The entries of $\mathbf{n}_m(f_k)/\sqrt{M\sigma_k^2}$ are independently, zero mean, and normally distributed with variance $1/M$. The normalized noise, $\mathbf{u}_k(\theta_1)$ and $\mathbf{v}_k$ will be utilized by the perturbed subspace theory and random matrix theory in Section III-A and III-B.

In the ISSM, the space spectrum is calculated by combining the resulting measurements for all the frequency bins equally [17], [18]. However, the SNR within each frequency bin of the wideband colored signal is different. The precision of DOA estimation from the data matrix changes from one frequency bin to another. We improve the ISSM by assigning optimal weights to different frequency bins and estimate the DOA as

$$\begin{aligned}\hat{\theta} &= \arg\min_{\theta} \sum_{k=1}^{K} w_k \underbrace{\mathbf{u}_k^H(\theta)\hat{\mathbf{U}}_k^{\perp}(\hat{\mathbf{U}}_k^{\perp})^H\mathbf{u}_k(\theta)}_{\hat{\psi}_k(\theta)} \\ &= \arg\min_{\theta} \sum_{k=1}^{K} w_k \mathbf{u}_k^H(\theta)\left[\mathbf{I} - \hat{\mathbf{u}}_k\hat{\mathbf{u}}_k^H\right]\mathbf{u}_k(\theta) \qquad (5) \\ &= \arg\max_{\theta} \sum_{k=1}^{K} w_k \underbrace{\mathbf{u}_k^H(\theta)\hat{\mathbf{u}}_k\hat{\mathbf{u}}_k^H\mathbf{u}_k(\theta)}_{\hat{\phi}_k(\theta)},\end{aligned}$$

where w_k is normalized such that $\sum_{k=1}^{K} w_k = 1$, and $\mathbf{u}_k(\theta) = \mathbf{a}_k(\theta)/\sqrt{N}$ is the normalized steering vector. All the weights $w_k, k \in [K]$ are chosen to be the same in the ISSM. We will deduce a method to compute the weights according to the parameters of each frequency bin in this paper.

The block diagram of the weighted incoherent signal subspace method is shown in Fig. 1. The signal from each sensor is partitioned and each partition is transformed to the frequency domain by DFT. The data at the same frequency from all the sensors are stacked in a subband snapshot vector. All the snapshot vectors at the same frequency are then stacked in a data matrix. The SVD is applied to each data matrix and the space spectrum of each frequency bin is obtained. The combined space spectrum is computed by weighting and accumulating the space spectrum of all the frequency bins. The DOA is estimated by locating the peak of the combined space spectrum.

III. PERFORMANCE OF DOA ESTIMATION FOR NARROWBAND SIGNALS

The mean square error (MSE) of DOA estimation is used to calculate the optimal weight. We will study two approaches to evaluate the DOA estimation for narrowband signals, one is the perturbed subspace based approach [24], [25], the other is the random matrix theory based approach [26]. The derivations of the two approaches are sketched here under the weighted multiple frequencies situation.

A. PERTURBED SUBSPACE BASED APPROACH

The perturbed subspace based approach handles $\hat{\mathbf{U}}_k^{\perp}$ as

$$\hat{\mathbf{U}}_k^{\perp} = \mathbf{U}_k^{\perp} + \Delta\mathbf{U}_k^{\perp}, \qquad (6)$$

where $\mathbf{U}_k^{\perp}$ is stacked by the left singular vectors of $\mathbf{A}_k\mathbf{S}_k$ associated with the zero singular values, and $\Delta\mathbf{U}_k^{\perp}$ is the perturbation in the estimated orthogonal subspace. Also, $\mathbf{U}_k^{\perp}$ is the orthogonal complement of the steering vector, i.e.,

$$\mathbf{u}_k^H(\theta_1)\mathbf{U}_k^{\perp} = \mathbf{0}. \qquad (7)$$

It is obtained by the perturbed subspace method that [24]

$$\Delta\mathbf{U}_k^{\perp} \doteq -\frac{1}{\sqrt{MNE_k}}\mathbf{u}_k(\theta_1)\mathbf{v}_k^H\mathbf{N}_k^H\mathbf{U}_k^{\perp}, \qquad (8)$$

where $\doteq$ means equal up to the first order terms.

The performance of DOA estimation is evaluated using the approximation of the perturbed subspace $\Delta\mathbf{U}_k^{\perp}$. The derivative of the objective function following the first equal sign in (5) should be zero at the estimate angle $\hat{\theta}_{\mathrm{PS}}$.

$$\sum_{k=1}^{K} w_k\hat{\psi}_k^{(1)}(\hat{\theta}_{\mathrm{PS}}) \triangleq \sum_{k=1}^{K} w_k \frac{\partial\hat{\psi}_k(\theta)}{\partial\theta}\bigg|_{\hat{\theta}_{\mathrm{PS}}} = 0. \qquad (9)$$

Denote $\Delta\theta_{\mathrm{PS}} = \hat{\theta}_{\mathrm{PS}} - \theta_1$ as the estimation error. Expanding $\sum_{k=1}^{K} w_k \hat{\psi}_k^{(1)}(\hat{\theta}_{\mathrm{PS}})$ around the real direction θ_1 using Taylor Series, we obtain

$$\sum_{k=1}^{K} w_k \hat{\psi}_k^{(1)}(\theta_1) + \sum_{k=1}^{K} w_k \hat{\psi}_k^{(2)}(\theta_1) \cdot \Delta\theta_{\mathrm{PS}} + o(\Delta\theta_{\mathrm{PS}}) = 0, \tag{10}$$

where $\hat{\psi}_k^{(1)}(\theta_1)$ indicates the first derivative of $\hat{\psi}_k(\theta_1)$, $\hat{\psi}_k^{(2)}(\theta_1)$ indicates the second, and $o(\Delta\theta_{\mathrm{PS}})$ means domination by $\Delta\theta_{\mathrm{PS}}$ asymptotically.

Neglecting the $o(\Delta\theta_{\mathrm{PS}})$ terms, we obtain

$$\Delta\theta_{\mathrm{PS}} = -\frac{\sum_{k=1}^{K} w_k \hat{\psi}_k^{(1)}(\theta_1)}{\sum_{k=1}^{K} w_k \hat{\psi}_k^{(2)}(\theta_1)}. \tag{11}$$

Evaluating the derivatives at θ_1 by differentiating $\hat{\psi}_k(\theta)$ with respect to θ, we have

$$\hat{\psi}_k^{(1)}(\theta_1) = 2\mathrm{Re}\left[\mathbf{u}_k^H(\theta_1)\hat{\mathbf{U}}_k^{\perp}(\hat{\mathbf{U}}_k^{\perp})^H\mathbf{u}_k^{(1)}(\theta_1)\right], \tag{12a}$$

and

$$\begin{aligned}\hat{\psi}_k^{(2)}(\theta_1) =& 2\mathrm{Re}\left[\mathbf{u}_k^H(\theta_1)\hat{\mathbf{U}}_k^{\perp}(\hat{\mathbf{U}}_k^{\perp})^H\mathbf{u}_k^{(2)}(\theta_1)\right] + \\ & 2\left\|(\hat{\mathbf{U}}_k^{\perp})^H\mathbf{u}_k^{(1)}(\theta_1)\right\|^2.\end{aligned} \tag{12b}$$

where $\mathrm{Re}[\cdot]$ is the function of taking the real part of a complex number, and $\|\cdot\|$ the ℓ_2 norm of a vector.

Substituting (6) into (12a) and keeping (7) in mind, we have

$$\hat{\psi}_k^{(1)}(\theta_1) = 2\mathrm{Re}\left[\mathbf{u}_k^H(\theta_1)\Delta\mathbf{U}_k^{\perp}(\mathbf{U}_k^{\perp})^H\mathbf{u}_k^{(1)}(\theta_1)\right], \tag{13}$$

where only the first order perturbation in $\Delta\mathbf{U}_k^{\perp}$ is kept.

The the first order perturbation of $\hat{\mathbf{U}}_k^{\perp}$ in $\Delta\mathbf{U}_k^{\perp}$ is neglected when approximating $\hat{\psi}_k^{(2)}(\theta_1)$, so that only the first order perturbation of $\hat{\mathbf{U}}_k^{\perp}$ remains in $\Delta\theta_{\mathrm{PS}}$. Then we have

$$\hat{\psi}_k^{(2)}(\theta_1) = 2\mathbf{u}_k^{(1)H}(\theta_1)\mathbf{U}_k^{\perp}(\mathbf{U}_k^{\perp})^H\mathbf{u}_k^{(1)}(\theta_1). \tag{14}$$

Substituting (8) into (13), we obtain

$$\hat{\psi}_k^{(1)}(\theta_1) = -2\mathrm{Re}\left[\boldsymbol{\zeta}_k^H\mathbf{N}_k^H\boldsymbol{\beta}_k\right], \tag{15}$$

where $\boldsymbol{\zeta}_k = \mathbf{v}_k\mathbf{u}_k^H(\theta_1)\mathbf{u}_k(\theta_1)/\sqrt{MNE_k} = \mathbf{v}_k/\sqrt{MNE_k}$, and $\boldsymbol{\beta}_k = \mathbf{U}_k^{\perp}(\mathbf{U}_k^{\perp})^H\mathbf{u}_k^{(1)}(\theta_1)$.

Substituting (15) and (14) into (11) and considering $\mathbf{u}_k^{(1)H}(\theta_1)\mathbf{U}_k^{\perp}(\mathbf{U}_k^{\perp})^H\mathbf{u}_k^{(1)}(\theta_1) = \|\boldsymbol{\beta}_k\|^2$, we have

$$\Delta\theta_{\mathrm{PS}} = \frac{\sum_{k=1}^{K} w_k\mathrm{Re}\left[\boldsymbol{\zeta}_k^H\mathbf{N}_k^H\boldsymbol{\beta}_k\right]}{\sum_{k=1}^{K} w_k\|\boldsymbol{\beta}_k\|^2}. \tag{16}$$

Considering the zero mean and independence of $\mathbf{N}_k$, we get the expectation $\mathbb{E}[\Delta\theta_{\mathrm{PS}}] = 0$, and the MSE

$$\mathbb{E}[\Delta\theta_{\mathrm{PS}}^2] = \frac{\sum_{k=1}^{K} w_k^2\|\boldsymbol{\zeta}_k\|^2\|\boldsymbol{\beta}_k\|^2\sigma_k^2}{2\left(\sum_{k=1}^{K} w_k\|\boldsymbol{\beta}_k\|^2\right)^2}, \tag{17}$$

where $\mathrm{var}\left[\mathrm{Re}\left[\boldsymbol{\zeta}_k^H\mathbf{N}_k^H\boldsymbol{\beta}_k\right]\right] = \frac{1}{2}\mathrm{var}\left[\boldsymbol{\zeta}_k^H\mathbf{N}_k^H\boldsymbol{\beta}_k\right]$ is utilized. Here $\mathrm{var}[\cdot]$ denotes taking the variance.

B. RANDOM MATRIX THEORY BASED APPROACH

Most estimation methods rely on the asymptotic statistics that the number of snapshots grows large relative to the sensor size, i.e., M/N tends to ∞. However, on encountering extremely large systems or systems requiring fast dynamics, which appear more and more frequently in modern signal processing, the M/N may not be large [27]. An effective tool to handle this arising problem is the large dimensional random matrix theory [28]. Large dimensional random matrix theory usually adopts a new asymptotic statistics that $M, N \to \infty$, and $N/M \to t \in (0, \infty)$ [29], [30]. For the asymptotic results, in theory, the infinite size of the matrix is required, which is infeasible in practice. However, the results are remarkably accurate, even for relatively moderate matrix sizes [31]. The new asymptotic statistics implies that the number of snapshots and the number of the sensors are of the same magnitude, which is much close to the practical situations, thus the result from the random theory is applicable more generally than that from the perturbed subspace theory.

The random matrix theory based approach calculates the MSE of DOA estimation by evaluating the inner product of the steering vector and the signal subspace in the regime that the dimensions of matrices increase at the same rate. In the random matrix theory, as $M, N \to \infty$, $N/M \to t \in (0, \infty)$,

$$\left|\langle\hat{\mathbf{u}}_k, \mathbf{u}_k(\theta_1)\rangle\right|^2 \xrightarrow{\text{a.s.}} \alpha_k^2 = \begin{cases} 1 - \frac{t(1+SNR_k)}{SNR_k(SNR_k+t)}, & \text{if } SNR_k > t^{1/2} \\ 0, & \text{otherwise} \end{cases} \tag{18}$$

where $\xrightarrow{\text{a.s.}}$ means almost sure convergence [32]. This phase transition phenomenon is an important result in large dimensional random matrix theory dealing with the spiked model. Equation (18) states that the sample singular vector is an informative estimate of the normalized steering vector only in the regime when the SNR is greater than some threshold. Furthermore, in this regime, the sample singular vector lies on a cone around the normalized steering vector, and the angle of the cone is determined by the array SNR and the constant *t*.

The inner product $\langle\hat{\mathbf{u}}_k, \mathbf{u}_k(\theta_1)\rangle$ appears in the objective function in (5) in the form of $\left|\langle\hat{\mathbf{u}}_k, \mathbf{u}_k(\theta_1)\rangle\right|^2$, which depends only on the magnitude of $\langle\hat{\mathbf{u}}_k, \mathbf{u}_k(\theta_1)\rangle$ and is invariant to its phase. Therefore, the performance may be carried out assuming $\langle\hat{\mathbf{u}}_k, \mathbf{u}_k(\theta_1)\rangle \in \mathbb{R}$ [26]. Then we have the approximation

$$\langle\hat{\mathbf{u}}_k, \mathbf{u}_k(\theta_1)\rangle \approx \alpha_k. \tag{19}$$

The results in (18) and (19) is about the inner product of the steering vector and the signal subspace. The objective function following the third equal sign in (5) is employed to leverage results from the random matrix theory. Differentiating the objective function with respect to θ and let the result be zero at the estimated $\hat{\theta}_{\mathrm{RMT}}$, we get

$$\Delta\theta_{\mathrm{RMT}} = -\frac{\sum_{k=1}^{K} w_k \hat{\phi}_k^{(1)}(\theta_1)}{\sum_{k=1}^{K} w_k \hat{\phi}_k^{(2)}(\theta_1)}, \tag{20}$$

where $\Delta\theta_{\mathrm{RMT}} = \hat{\theta}_{\mathrm{RMT}} - \theta_1$.

Evaluating the derivatives at θ_1 by differentiating $\hat{\phi}_k$ with respect to θ, we have

$$\hat{\phi}_k^{(1)}(\theta_1) = 2\mathrm{Re}\left[\mathbf{u}_k^H(\theta_1)\hat{\mathbf{u}}_k\hat{\mathbf{u}}_k^H\mathbf{u}_k^{(1)}(\theta_1)\right], \tag{21a}$$

$$\hat{\phi}_k^{(2)}(\theta_1) = 2\mathrm{Re}\left[\mathbf{u}_k^H(\theta_1)\hat{\mathbf{u}}_k\hat{\mathbf{u}}_k^H\mathbf{u}_k^{(2)}(\theta_1)\right] + 2\left|\hat{\mathbf{u}}_k^H\mathbf{u}_k^{(1)}(\theta_1)\right|^2. \tag{21b}$$

Decomposing the derivatives of steering vector in the signal subspace and orthogonal to it, we have

$$\mathbf{u}_k^{(1)}(\theta_1) = \gamma_{1,k}\mathbf{u}_k(\theta_1) + \delta_{1,k}\mathbf{u}_k^{\perp}(\theta_1), \tag{22a}$$

$$\mathbf{u}_k^{(2)}(\theta_1) = \gamma_{2,k}\mathbf{u}_k(\theta_1) + \delta_{2,k}\mathbf{u}_k^{\perp}(\theta_1), \tag{22b}$$

where $\mathbf{u}_k(\theta_1)^{\perp}$ is a basis vector of the subspace orthogonal to the signal subspace which makes $\delta_{1,k}$ and $\delta_{2,k}$ real numbers. Then

$$\gamma_{1,k} = \mathbf{u}_k^H(\theta_1)\mathbf{u}_k^{(1)}(\theta_1), \tag{23a}$$

$$\gamma_{2,k} = \mathbf{u}_k^H(\theta_1)\mathbf{u}_k^{(2)}(\theta_1), \tag{23b}$$

$$\delta_{1,k}^2 = \left\|\mathbf{u}_k^{(1)}(\theta_1)\right\|^2 - |\gamma_{1,k}|^2, \tag{23c}$$

$$\delta_{2,k}^2 = \left\|\mathbf{u}_k^{(2)}(\theta_1)\right\|^2 - |\gamma_{2,k}|^2. \tag{23d}$$

Similar to the inner product in (18), it is given by random matrix theory [26] that as $M, N \to \infty$, $N/M \to t \in (0, \infty)$,

$$\mathbb{E}\left[\mathrm{Re}\left[\sqrt{N}\hat{\mathbf{u}}_k^H\mathbf{u}_k^{\perp}(\theta_1)\right]^2\right] \xrightarrow{\text{a.s.}} \frac{1-\alpha_k^2}{2}. \tag{24}$$

Note that the basis vector $\mathbf{u}_k^{\perp}(\theta_1)$ is usually different in (22a) and (22b), however, $\mathbb{E}\left[\mathrm{Re}\left[\sqrt{N}\hat{\mathbf{u}}_k^H\mathbf{u}_k^{\perp}(\theta_1)\right]^2\right]$ remains the same for every basis vector in the subspace orthogonal to the signal subspace [26]. Therefore, the same symbol $\mathbf{u}_k^{\perp}(\theta_1)$ is utilized for simplicity.

The vector $\mathbf{u}_k(\theta_1)$ is normalized, then $\mathbf{u}_k^H(\theta_1)\mathbf{u}_k(\theta_1) = 1$. Differentiating both sides of this equation with respect to θ_1, we get

$$\mathrm{Re}\left[\mathbf{u}_k^H(\theta_1)\mathbf{u}_k^{(1)}(\theta_1)\right] = \mathrm{Re}\left[\gamma_{1,k}\right] = 0. \tag{25}$$

Differentiating (25) again with respect to θ_1, we obtain

$$\mathrm{Re}\left[\mathbf{u}_k^H(\theta_1)\mathbf{u}_k^{(2)}(\theta_1)\right] + \left\|\mathbf{u}_k^{(1)}(\theta_1)\right\|^2 = 0. \tag{26}$$

Substituting (23b) and (23c) gives

$$|\gamma_{1,k}|^2 + \mathrm{Re}\left[\gamma_{2,k}\right] = -\delta_{1,k}^2. \tag{27}$$

Substituting (22a) into (21a) and applying (19) and (25), we obtain

$$\begin{aligned}\hat{\phi}_k^{(1)}(\theta_1) =& 2\mathrm{Re}\left[\gamma_{1,k}\right]\left|\mathbf{u}_k^H(\theta_1)\hat{\mathbf{u}}_k\right|^2 + \\ & 2\delta_{1,k}\mathrm{Re}\left[\mathbf{u}_k^H(\theta_1)\hat{\mathbf{u}}_k\hat{\mathbf{u}}_k^H\mathbf{u}_k^{\perp}(\theta_1)\right] \\ \approx& 2\delta_{1,k}\alpha_k\mathrm{Re}\left[\hat{\mathbf{u}}_k^H\mathbf{u}_k^{\perp}(\theta_1)\right].\end{aligned} \tag{28}$$

Squaring (28) and taking expectation, we obtain

$$\mathbb{E}\left[\left(\hat{\phi}_k^{(1)}(\theta_1)\right)^2\right] \approx \frac{2}{N}\delta_{1,k}^2\alpha_k^2(1-\alpha_k^2), \tag{29}$$

Similarly,

$$\begin{aligned}&\mathrm{Re}\left[\mathbf{u}_k^H(\theta_1)\hat{\mathbf{u}}_k\hat{\mathbf{u}}_k^H\mathbf{u}_k^{(2)}(\theta_1)\right] \\ =&\mathrm{Re}\left[\gamma_{2,k}\right]\left|\mathbf{u}_k^H(\theta_1)\hat{\mathbf{u}}_k\right|^2 + \delta_{2,k}\mathrm{Re}\left[\mathbf{u}_k^H(\theta_1)\hat{\mathbf{u}}_k\hat{\mathbf{u}}_k^H\mathbf{u}_k^{\perp}(\theta_1)\right] \\ \approx&\mathrm{Re}\left[\gamma_{2,k}\right]\alpha_k^2 + \delta_{2,k}\alpha_k\mathrm{Re}\left[\hat{\mathbf{u}}_k^H\mathbf{u}_k^{\perp}(\theta_1)\right].\end{aligned} \tag{30}$$

Applying (22a) into $\left|\hat{\mathbf{u}}_k^H\mathbf{u}_k^{(1)}(\theta_1)\right|^2$ gives

$$\begin{aligned}\left|\hat{\mathbf{u}}_k^H\mathbf{u}_k^{(1)}(\theta_1)\right|^2 =& |\gamma_{1,k}|^2\left|\hat{\mathbf{u}}_k^H\mathbf{u}_k(\theta_1)\right|^2 + \delta_{1,k}^2\left|\hat{\mathbf{u}}_k^H\mathbf{u}_k^{\perp}(\theta_1)\right|^2 + \\ & 2\delta_{1,k}\mathrm{Re}\left[\gamma_{1,k}\hat{\mathbf{u}}_k^H\mathbf{u}_k(\theta_1)\hat{\mathbf{u}}_k^H\mathbf{u}_k^{\perp}(\theta_1)\right] \\ \approx& |\gamma_{1,k}|^2\alpha_k^2 + \delta_{1,k}^2\left|\hat{\mathbf{u}}_k^H\mathbf{u}_k^{\perp}(\theta_1)\right|^2 + \\ & 2\delta_{1,k}\alpha_k\mathrm{Re}\left[\gamma_{1,k}\hat{\mathbf{u}}_k^H\mathbf{u}_k^{\perp}(\theta_1)\right].\end{aligned} \tag{31}$$

Substituting (30) and (31) into (21b) and retaining only the dominant part, we obtain [26]

$$\hat{\phi}_k^{(2)}(\theta_1) \approx 2\mathrm{Re}\left[\gamma_{2,k}\right]\alpha_k^2 + 2|\gamma_{1,k}|^2\alpha_k^2 = -2\delta_{1,k}^2\alpha_k^2, \tag{32}$$

where (27) is used.

Considering the first order approximation of $\hat{\mathbf{u}}_k^H$ around $\mathbf{u}_k^H$ as in [24] and the orthogonality between $\mathbf{u}_k^H$ and $\mathbf{u}_k^{\perp}(\theta_1)$, we have $\mathbb{E}\left[\hat{\phi}_k^{(1)}(\theta_1)\right] \approx 0$ in the light of (28). The noises within each frequency bin is independent of each other. As a function of the noise within the kth frequency bin only, $\hat{\phi}_k^{(1)}(\theta_1), k \in [K]$, is also independent of each other. By applying (32) and (29), we obtain

$$\mathbb{E}[\Delta\theta_{RMT}^2] = \frac{\sum_{k=1}^{K} w_k^2\delta_{1,k}^2\alpha_k^2(1-\alpha_k^2)}{2N\left(\sum_{k=1}^{K} w_k\delta_{1,k}^2\alpha_k^2\right)^2}. \tag{33}$$

IV. METHODS FOR WEIGHTING SPACE SPECTRUM

The MSE of DOA estimation for wideband signals is a function of the weight for each frequency bin. The weight can be computed by minimizing the MSE. Leveraging the deduced MSE, we have following two theorems.

Theorem 1: The weight minimizing the estimation MSE deduced by the perturbed subspace based approach is

$$\hat{w}_k^{\mathrm{PS}} = \frac{1}{\sum_{k=1}^{K} SNR_k}SNR_k,\ k \in [K]. \tag{34}$$

The derivation of Theorem 1 can be found in APPENDIX A.

Theorem 2: The weight minimizing the estimation MSE deduced by the random matrix theory based approach is

$$\hat{w}_k^{\mathrm{RMT}} = \frac{1}{\sum_{k=1}^{K} \frac{1}{1-\alpha_k^2}} \frac{1}{1-\alpha_k^2},\ k \in [K]. \tag{35}$$

The derivation of Theorem 2 can be found in APPENDIX B.

As the SNR_k approaches $t^{1/2}$ from above, the limit of α_k^2 is 0. Therefore, α_k^2 is continuous as a function of SNR_k. It should be noted that, if $SNR_k \leq t^{1/2}$, then $\alpha_k^2 = 0$, and $\mathbb{E}[\Delta\theta_{RMT}^2]$ tends to infinity. For $SNR_k = t^{1/2} + \epsilon$ with ϵ being any positive number, $\alpha_k^2 > 0$. The weight minimizing the MSE derived from the random matrix theory based approach is calculated by $1/(1-\alpha_k^2)$ followed by normalization according to Theorem 2. When α_k^2 approaches 0, we can also use $1/(1-\alpha_k^2)$ as the weight before normalization. Therefore, we leverage (35) as the weight for any SNR_k. If the array SNR for the kth frequency bin is less than $t^{1/2}$, α_k^2 equals to zero, then $1/(1-\alpha_k^2)$ constantly equals to 1. This means that the optimal weight of a frequency bin does not change with SNR if the SNR of the frequency bin is less than a certain threshold. This is different from most conventional methods, in which the weight will continuously vary with respect to some parameters, such as the SNR.

It can be seen from (18) that $\hat{w}_k^{\mathrm{PS}}$ approximately equals to $\hat{w}_k^{\mathrm{RMT}}$ when the array SNR is high and the ratio between the number of snapshots and the number of array sensors is large. The comparison between the perturbed subspace based method and the random matrix theory based method will be further studied in Section V.

As for the situation of multiple sources, we can focus on each source respectively. The weighting method can be applied to each source and then the DOA of the source can be calculated as the approach for the situation with single source. This process is repeated until all the DOAs are estimated. However, this method is subjected to heavy computational loading and requires preliminary knowledge of DOAs. As an alternative, the optimal weighting can be applied to each direction, since there is usually at most one source at each direction. We calculate weights for each frequency bin and accumulate them at each hypothesized DOA to obtain the space spectrum function, then estimate DOAs by locating the peaks of the space spectrum function. This method does not require preliminary knowledge for DOAs.

When calculating the weights at each direction, we need the array SNR at certain direction, which can be calculated by the signal after beamforming at this direction. For example, the array SNR at direction θ within the kth frequency bin can be estimated as

$$SNR_k(\theta) = \frac{\max\left(\mathbf{a}_k(\theta)^H \mathbf{X}_k \mathbf{X}_k^H \mathbf{a}_k(\theta) - MN\hat{\sigma}_k^2,\ 0\right)}{MN\hat{\sigma}_k^2}. \tag{36}$$

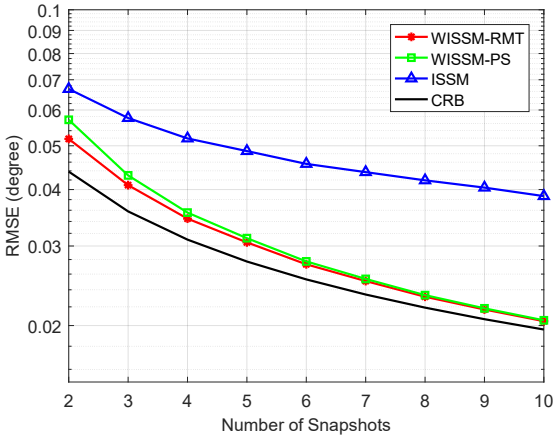

FIGURE 2. The performance comparison among the proposed weighted methods and the ISSM. The far-field sources located at 11° and 17°. The number of sensors was 30. The number of frequency bins was 10. The sensor SNR was uniformly distributed from -10dB to 10dB.

where $\hat{\sigma}_k^2$ is the noise power within the kth frequency bin predicted from the received data without any source signal.

The steps of the scheme is described as follows.

1) Divide the sensor signal into M segments and compute the temporal DFT of each segment.

2) Form $\mathbf{X}_k,\ k \in [K]$ and apply SVD to $\mathbf{X}_k$. Sort the singular values of $\mathbf{X}_k$ in decreasing order.

3) For each hypothesized DOA θ, calculate the array SNR according to (36), and the optimal weight $\hat{w}_k(\theta)$ of each frequency bin according to (34) or (35). Then the spectrum function is obtained:

$$P(\theta) = \sum_{k=1}^{K} \sum_{q=1}^{Q} \hat{w}_k(\theta) \mathbf{a}_k^H(\theta) \hat{\mathbf{u}}_{k,q} \hat{\mathbf{u}}_{k,q}^H \mathbf{a}_k(\theta), \tag{37}$$

where $\hat{\mathbf{u}}_{k,q}$ is the left singular vector corresponding to the qth singular value of $\mathbf{X}_k$.

4) Estimate DOAs by locating the peaks of $P(\theta)$.

V. NUMERICAL RESULTS

We test the proposed weighted incoherent signal subspace method (WISSM) using Monte Carlo simulations. A uniform linear array composes of 30 sensors received the signals radiated by two far-field independent Gaussian sources located at 11° and 17° respectively. The frequency of the sources ranged from 95MHz to 105MHz. The sensor spacing was half the wavelength corresponding to the highest frequency. The DFT was performed using 10 frequency bins. The variance of the noise within all the frequency bins was set to 1. The weighted incoherent signal subspace method using the weight in (34) was denoted as WISSM-PS and the algorithm leveraging the weight in (35) was denoted as WISSM-RMT.

Fig.2 shows the root mean square error (RMSE) of the WISSM-RMT, the WISSM-PS, and the ISSM with respect

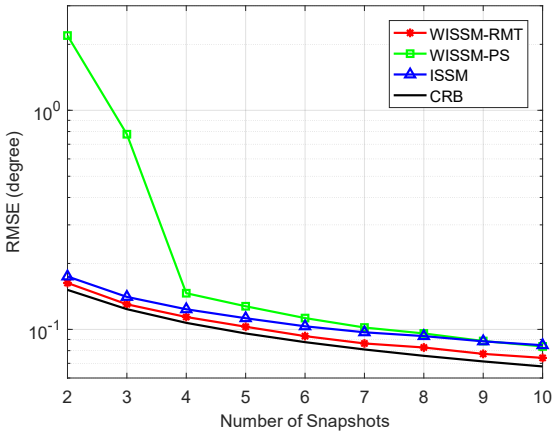

FIGURE 3. The performance comparison among the proposed weighted methods and the ISSM. The far-field sources located at 11° and 17°. The number of sensors was 30. The number of frequency bins was 10. The sensor SNR was uniformly distributed from -20dB to 0dB.

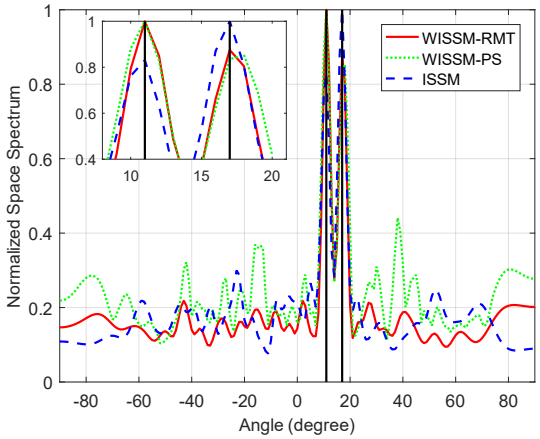

FIGURE 4. The normalized spacial spectrum of the proposed weighted methods and the ISSM. The far-field sources located at 11° and 17°. The number of sensors was 30. The number of frequency bins was 10. The sensor SNR was uniformly distributed from -20dB to 0dB. The number of snapshots was 2.

to the number of snapshots. The Cramér-Rao bound (CRB) [23] is also shown. The RMSE is defined as

$$\text{RMSE} \triangleq \sqrt{\frac{1}{I}\frac{1}{Q}\sum_{i=1}^{I}\sum_{q=1}^{Q}\left(\hat{\theta}_q^i - \theta_q\right)^2}, \qquad (38)$$

where I is the number of trials and $\hat{\theta}_q^i$ denotes the estimate of θ_q in the ith trial. The senor SNR is defined by $SNR'_{k,q} = 10\log[E_{k,q}/\sigma_k^2]$, which is the SNR of each source signal at a single sensor, with log representing the logarithm to base 10 in this paper. The sensor SNR was uniformly distributed from -10dB to 10dB in Fig. 2. Each RMSE in Fig. 2 was evaluated by 10000 trials.

It can be seen from Fig.2 that the WISSM-RMT performs better than the ISSM. At small number of snapshots, the RMSE of the WISSM-RMT is smaller than that of the WISSM-PS. The superiority of the WISSM-RMT comes from the usage of the results from random matrix theory. As the number of snapshots increases, the RMSEs of the WISSM-RMT and the WISSM-PS tend to close to each other. The reason is that the weights of the WISSM-RMT are approximately equal to the weights of the WISSM-PS while the number of snapshots is large. The weights of the WISSM-PS will fail under the condition at low SNR and with few snapshots, which does not agree with the approximation condition of the perturbed subspace method.

The performance comparison among the WISSM-RMT, the WISSM-PS, and the ISSM under the condition at low SNR and with few snapshots is demonstrated in Fig. 3, where the simulation conditions were the same as that in Fig. 2, except the sensor SNR uniformly distributed from -20dB to 0dB. It can be seen from Fig. 3 that the WISSM-PS even performs worse than the ISSM at small number of snapshots. While the WISSM-RMT works well under both the conditions set in Fig. 2 and Fig. 3. The reason is that the random matrix theory adopting the regime that the number of snapshots and the number of sensors are comparable in magnitude, which is more general and more consistent with the actual situation than the regime adopted by the perturbed subspace theory, so that the the random matrix theory is more extensively applicable. Equation (35) and (18) reveal that those frequency bins with SNR less than some threshold are weighted equally according to the random matrix theory. Therefore, the ISSM with equal weights performs better than the WISSM-PS with weights proportional to SNR under the condition at low SNR and with few snapshots.

To further reveal the algorithm performance, an example run of the normalized spacial spectrum for the WISSM-RMT, the WISSM-PS, and the ISSM is shown in Fig. 4, where the sensor SNR was uniformly distributed from -20dB to 0dB and the number of snapshots was fixed to 2. The two vertical lines indicate the directions of the two far-field sources. The WISSM-RMT and the ISSM can distinguish the two sources successfully. Whereas The peak of the space spectrum around 17° for the WISSM-PS locates at a bias angle. The amplitude of the peaks locate away from the source direction are also quite high, which can be even larger than the amplitude of true peaks at high risk.

Considering the superiority of the WISSM-RMT to the WISSM-PS, we only compare the WISSM-RMT with other algorithms for wideband DOA estimation, which is shown in Fig. 5. The simulation conditions are the same as that shown in Fig. 2. In the simulations of WAVES, the initial value was generated from perturbations of the true DOAs by adding zero mean Gaussian random noise, the variance of which equaled to the CRB. Fig. 5 also demonstrates that all the methods perform better as the number of snapshots increases. The TOPS is more sensitive to the number of snapshots, and is applicable to scenarios where there is considerable number of snapshots. The initial values show as an important factor that impacts the performance of WAVES. When the

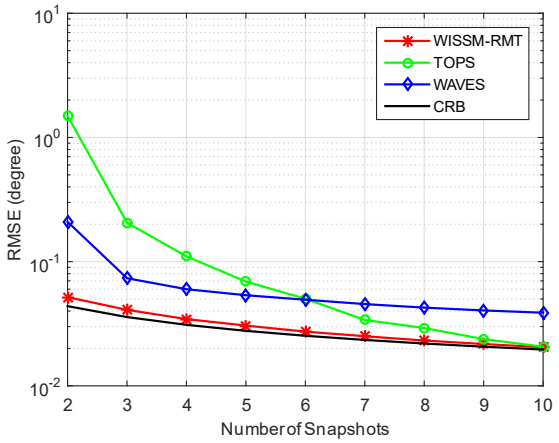

FIGURE 5. Estimation performance of different wideband DOA algorithms. The far-field sources located at degrees of 11° and 17°. The number of sensors was 30. The number of frequency bins was 10. The sensor SNR was uniformly distributed from -10dB to 10dB.

number of snapshots is small, the error of the initial values increases, which degrades the performance of the WAVES. The WISSM-RMT approaches the CRB well, and shows better performance than the other algorithms, especially in the regime of relative few snapshots.

VI. CONCLUSION

This paper presents two methods which are used for DOA estimation on wideband colored signals. The perturbed subspace based method is concise in computing the weights and performs well at high SNR and with adequate snapshots. The random matrix theory based method shows better estimation precision than the perturbed subspace based method, especially in the regime at low SNR and with few snapshots. The performance of the random matrix theory based method is guaranteed by using insights from the large dimensional random matrix theory. The proposed methods do not need initial values and is competent to the DOA estimation on wideband colored signals.

.

APPENDIX A DERIVATION OF THEOREM 1

Denote $\mathbf{w} = [w_1, ..., w_K]^T$, $\mathbf{b} = [\|\boldsymbol{\beta}_1\|, ..., \|\boldsymbol{\beta}_K\|]^T$, $\mathbf{H} = \text{diag}\left([\|\boldsymbol{\zeta}_1\|\sigma_1, ..., \|\boldsymbol{\zeta}_K\|\sigma_K]\right)$ and $\tilde{\mathbf{w}} = \mathbf{H}(\mathbf{w} \circ \mathbf{b})$, where $\circ$ denotes Hadamard product, we have

$$\mathbb{E}[\Delta\theta^2_{\text{PS}}] = \frac{\tilde{\mathbf{w}}^T\tilde{\mathbf{w}}}{2\tilde{\mathbf{w}}^T(\mathbf{H}^{-1})^T\mathbf{b}\mathbf{b}^T\mathbf{H}^{-1}\tilde{\mathbf{w}}}. \tag{39}$$

The weight to minimize $\mathbb{E}[\Delta\theta^2_{\text{PS}}]$ is shown as

$$\begin{aligned}\hat{\mathbf{w}} &= \arg\min_{\mathbf{w}} \mathbb{E}[\Delta\theta^2_{PS}] \\ &= \arg\max_{\mathbf{w}} \underbrace{\left(\frac{\tilde{\mathbf{w}}}{\|\tilde{\mathbf{w}}\|}\right)^T (\mathbf{H}^{-1})^T\mathbf{b}\mathbf{b}^T\mathbf{H}^{-1}\left(\frac{\tilde{\mathbf{w}}}{\|\tilde{\mathbf{w}}\|}\right)}_{T(\tilde{\mathbf{w}})},\end{aligned} \tag{40}$$

which is a quadratic form restricted to the unit sphere in some coordinate system.

Let $\mathbf{y} = \tilde{\mathbf{w}}/\|\tilde{\mathbf{w}}\|$. The maximization of $T(\tilde{\mathbf{w}})$ becomes

$$\max \mathbf{y}^T(\mathbf{H}^{-1})^T\mathbf{b}\mathbf{b}^T\mathbf{H}^{-1}\mathbf{y},\ s.t.\ \mathbf{y}^T\mathbf{y} = 1. \tag{41}$$

By using the method of Lagrange multipliers and solving the first derivative condition, the optimal unit-norm $\hat{\mathbf{y}}$ satisfies

$$(\mathbf{H}^{-1})^T\mathbf{b}\mathbf{b}^T\mathbf{H}^{-1}\hat{\mathbf{y}} = \nu_1\hat{\mathbf{y}}, \tag{42}$$

where ν_1 is the Lagrange multiplier, and $\hat{\mathbf{y}}$ is an eigenvector of $(\mathbf{H}^{-1})^T\mathbf{b}\mathbf{b}^T\mathbf{H}^{-1}$ associated with the eigenvalue ν_1. Then

$$\hat{\mathbf{y}}^T(\mathbf{H}^{-1})^T\mathbf{b}\mathbf{b}^T\mathbf{H}^{-1}\hat{\mathbf{y}} = \nu_1\hat{\mathbf{y}}^T\hat{\mathbf{y}} = \nu_1. \tag{43}$$

Therefore, $T(\tilde{\mathbf{w}})$ is bounded by the extreme eigenvalues of $(\mathbf{H}^{-1})^T\mathbf{b}\mathbf{b}^T\mathbf{H}^{-1}$, which is a real symmetric matrix with rank one. The eigenvector associated with the maximum eigenvalue maximizes $T(\tilde{\mathbf{w}})$.

Multiplying $(\mathbf{H}^{-1})^T\mathbf{b}\mathbf{b}^T\mathbf{H}^{-1}$ by $(\mathbf{H}^{-1})^T\mathbf{b}$, we obtain

$$(\mathbf{H}^{-1})^T\mathbf{b}\mathbf{b}^T\mathbf{H}^{-1}(\mathbf{H}^{-1})^T\mathbf{b} = \mathbf{b}^T\mathbf{H}^{-2}\mathbf{b}\cdot(\mathbf{H}^{-1})^T\mathbf{b}. \tag{44}$$

where the $\mathbf{b}^T\mathbf{H}^{-2}\mathbf{b}$ is a scalar. It is implied in (44) that $(\mathbf{H}^{-1})^T\mathbf{b}$ is an eigenvector of $(\mathbf{H}^{-1})^T\mathbf{b}\mathbf{b}^T\mathbf{H}^{-1}$ corresponding to the eigenvalue $\mathbf{b}^T\mathbf{H}^{-2}\mathbf{b}$, which is an eigenvalue larger than zero and therefore is the maximum one. Then

$$T(\tilde{\mathbf{w}}) \le \mathbf{b}^T\mathbf{H}^{-2}\mathbf{b}. \tag{45}$$

When $\tilde{\mathbf{w}} = \kappa_1\cdot(\mathbf{H}^{-1})^T\mathbf{b}$, $T(\tilde{\mathbf{w}})$ reaches its maximum, where κ_1 is a constant. Replacing $\tilde{\mathbf{w}}$ with $\mathbf{H}(\mathbf{w}\circ\mathbf{b})$, we obtain the optimal weighting coefficient

$$\hat{w}_k^{PS} \propto \frac{1}{\|\boldsymbol{\zeta}_k\|^2\sigma_k^2}. \tag{46}$$

Considering the normalization and $\|\boldsymbol{\zeta}_k\|^2 = \frac{1}{MNE_k}$, we obtain (34).

APPENDIX B DERIVATION OF THEOREM 2

Denote $\mathbf{w} = [w_1, ..., w_K]^T$, $\mathbf{b} = [\delta_{1,1}\alpha_1, ..., \delta_{1,K}\alpha_K]^T$, $\mathbf{H} = \text{diag}\left(\left[\sqrt{1-\alpha_1^2}, ..., \sqrt{1-\alpha_K^2}\right]\right)$ and $\tilde{\mathbf{w}} = \mathbf{H}(\mathbf{w}\circ\mathbf{b})$, we have

$$\mathbb{E}[\Delta\theta^2_{RMT}] = \frac{\tilde{\mathbf{w}}^T\tilde{\mathbf{w}}}{2N\tilde{\mathbf{w}}^T(\mathbf{H}^{-1})^T\mathbf{b}\mathbf{b}^T\mathbf{H}^{-1}\tilde{\mathbf{w}}}. \tag{47}$$

The weight to minimize $\mathbb{E}[\Delta\theta^2_{RMT}]$ is shown as

$$\begin{aligned}\hat{\mathbf{w}} &= \arg\min_{\mathbf{w}} \mathbb{E}[\Delta\theta^2_{RMT}] \\ &= \arg\max_{\mathbf{w}} \underbrace{\left(\frac{\tilde{\mathbf{w}}}{\|\tilde{\mathbf{w}}\|}\right)^T (\mathbf{H}^{-1})^T\mathbf{b}\mathbf{b}^T\mathbf{H}^{-1}\left(\frac{\tilde{\mathbf{w}}}{\|\tilde{\mathbf{w}}\|}\right)}_{T(\tilde{\mathbf{w}})}.\end{aligned} \tag{48}$$

Similar to the computation in APPENDIX A, we obtain

$$T(\tilde{\mathbf{w}}) \le \mathbf{b}^T\mathbf{H}^{-2}\mathbf{b}. \tag{49}$$

When $\tilde{\mathbf{w}} = \kappa_2\cdot(\mathbf{H}^{-1})^T\mathbf{b}$, $T(\tilde{\mathbf{w}})$ reaches its maximum, where κ_2 is a constant. Replacing $\tilde{\mathbf{w}}$ by $\mathbf{H}(\mathbf{w}\circ\mathbf{b})$, we have

$$\hat{w}_k^{RMT} \propto \frac{1}{1-\alpha_k^2}. \tag{50}$$

Subject to the normalization, (35) is then obtained.

REFERENCES

[1] F. Rusek, D. Persson, B. K. Lau, E. G. Larsson, T. L. Marzetta, O. Edfors, and F. Tufvesson, "Scaling up mimo: Opportunities and challenges with very large arrays," IEEE Signal Process. Mag., vol. 30, no. 1, pp. 40–60, Jan. 2013.

[2] G. Han, L. Wan, L. Shu, and N. Feng, "Two novel DOA estimation approaches for real-time assistant calibration systems in future vehicle industrial," IEEE Syst. J., vol. 11, no. 3, pp. 1361–1372, Sep. 2017.

[3] Q. Yuan, Q. Chen, and K. Sawaya, "Accurate DOA estimation using array antenna with arbitrary geometry," IEEE Trans. Antennas Propag., vol. 53, no. 4, pp. 1352–1357, Apr. 2005.

[4] A. Liu, X. Zhang, Q. Yang, and W. Deng, "Fast DOA estimation algorithms for sparse uniform linear array with multiple integer frequencies," IEEE Access, vol. 6, pp. 29 952–29 965, May 2018.

[5] R. Schmidt, "Multiple emitter location and signal parameter estimation," IEEE Trans. Antennas Propag., vol. 34, no. 3, pp. 276–280, Mar. 1986.

[6] J. Chen, S. Guan, Y. Tong, and L. Yan, "Two-dimensional direction of arrival estimation for improved archimedean spiral array with MUSIC algorithm," IEEE Access, vol. 6, pp. 49 740–49 745, Aug. 2018.

[7] B. Liu, G. Gui, S. Matsushita, and L. Xu, "Dimension-reduced direction-of-arrival estimation based on $\ell_{2,1}$-norm penalty," IEEE Access, vol. 6, pp. 44 433–44 444, Aug. 2018.

[8] M. Li and Y. Lu, "Maximum likelihood doa estimation in unknown colored noise fields," IEEE Trans. Aerosp. Electron. Syst., vol. 44, no. 3, pp. 1079–1090, Jul. 2008.

[9] R. Roy and T. Kailath, "ESPRIT-estimation of signal parameters via rotational invariance techniques," IEEE Trans. Acoust., Speech, Signal Process., vol. 37, no. 7, pp. 984–995, Jul. 1989.

[10] J. Li, "DOA tracking in time-varying underwater acoustic communication channels," in OCEANS 2017 - Aberdeen, Jun. 2017, pp. 1–9.

[11] H. Chen and J. Zhao, "Coherent signal-subspace processing of acoustic vector sensor array for DOA estimation of wideband sources," Signal Process., vol. 85, no. 4, pp. 837–847, Apr. 2005.

[12] M. A. Doron and A. J. Weiss, "On focusing matrices for wide-band array processing," IEEE Trans. Signal Process., vol. 40, no. 6, pp. 1295–1302, Jun. 1992.

[13] E. D. Di Claudio and R. Parisi, "Waves: weighted average of signal subspaces for robust wideband direction finding," IEEE Trans. Signal Process., vol. 49, no. 10, pp. 2179–2191, Oct. 2001.

[14] B. Friedlander and A. J. Weiss, "Direction finding for wide-band signals using an interpolated array," IEEE Trans. Signal Process., vol. 41, no. 4, pp. 1618–1634, Apr. 1993.

[15] M. A. Doran, E. Doron, and A. J. Weiss, "Coherent wide-band processing for arbitrary array geometry," IEEE Trans. Signal Process., vol. 41, no. 1, pp. 414–417, Jan. 1993.

[16] Y.-S. Yoon, L. Kaplan, and J. McClellan, "Tops: new DOA estimator for wideband signals," IEEE Trans. Signal Process., vol. 54, no. 6, pp. 1977–1989, Jun. 2006.

[17] M. Wax, T.-J. Shan, and T. Kailath, "Spatio-temporal spectral analysis by eigenstructure methods," IEEE Trans. Acoust., Speech, Signal Process., vol. 32, no. 4, pp. 817–827, Aug. 1984.

[18] K. Han and A. Nehorai, "Wideband gaussian source processing using a linear nested array," IEEE Signal Process. Lett., vol. 20, no. 11, pp. 1110–1113, Nov. 2013.

[19] M. A. Doron, A. J. Weiss, and H. Messer, "Maximum-likelihood direction finding of wide-band sources," IEEE Trans. Signal Process., vol. 41, no. 1, pp. 411–414, Jan. 1993.

[20] B. Ottersten and T. Kailath, "Direction-of-arrival estimation for wide-band signals using the esprit algorithm," IEEE Trans. Acoust., Speech, Signal Process., vol. 38, no. 2, pp. 317–327, Feb. 1990.

[21] Q. Shen, W. Liu, W. Cui, S. Wu, Y. D. Zhang, and M. G. Amin, "Focused compressive sensing for underdetermined wideband DOA estimation exploiting high-order difference coarrays," IEEE Signal Process. Lett., vol. 24, no. 1, pp. 86–90, Jan. 2017.

[22] L. Wan, X. Kong, and F. Xia, "Joint range-Doppler-angle estimation for intelligent tracking of moving aerial targets," IEEE Internet Things J., vol. 5, no. 3, pp. 1625–1636, Jun. 2018.

[23] Z.-Q. He, Z.-P. Shi, L. Huang, and H. C. So, "Underdetermined DOA estimation for wideband signals using robust sparse covariance fitting," IEEE Signal Process. Lett., vol. 22, no. 4, pp. 435–439, Apr. 2015.

[24] F. Li, H. Liu, and R. Vaccaro, "Performance analysis for DOA estimation algorithms: unification, simplification, and observations," IEEE Trans. Aerosp. Electron. Syst., vol. 29, no. 4, pp. 1170–1184, Oct. 1993.

[25] F. Li and R. Vaccaro, "Analysis of min-norm and MUSIC with arbitrary array geometry," IEEE Trans. Aerosp. Electron. Syst., vol. 26, no. 6, pp. 976–985, Nov. 1990.

[26] R. Suryaprakash and R. Nadakuditi, "Consistency and mse performance of MUSIC-based DOA of a single source in white noise with randomly missing data," IEEE Trans. Signal Process., vol. 63, no. 18, pp. 4756–4770, Sep. 2015.

[27] R. Couillet and M. Debbah, "Signal processing in large systems: A new paradigm," IEEE Signal Process. Mag., vol. 30, no. 1, pp. 24–39, Jan. 2013.

[28] X. He, L. Chu, R. C. Qiu, Q. Ai, and Z. Ling, "A novel data-driven situation awareness approach for future gridsałusing large random matrices for big data modeling," IEEE Access, vol. 6, pp. 13 855–13 865, Mar. 2018.

[29] P. Vallet, X. Mestre, and P. Loubaton, "Performance analysis of an improved MUSIC DoA estimator," IEEE Trans. Signal Process., vol. 63, no. 23, pp. 6407–6422, Dec. 2015.

[30] D. Vazquez-Padin, F. Perez-Gonzalez, and P. Comesana-Alfaro, "A random matrix approach to the forensic analysis of upscaled images," IEEE Trans. Inf. Forensics Security, vol. 12, no. 9, pp. 2115–2130, Sep. 2017.

[31] X. He, Q. Ai, R. C. Qiu, W. Huang, L. Piao, and H. Liu, "A big data architecture design for smart grids based on random matrix theory," IEEE Trans. Smart Grid, vol. 8, no. 2, pp. 674-686, Mar. 2017.

[32] F. Benaych-Georges and R. R. Nadakuditi, "The singular values and vectors of low rank perturbations of large rectangular random matrices," J. Multivar. Anal., vol. 111, no. 5, pp. 120 – 135, Oct. 2012.

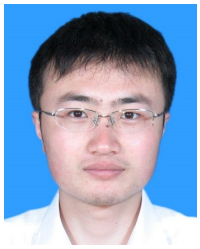

YECHAO BAI received the B.S. degree and the Ph.D. degree in electronic science and engineering from Nanjing University, Nanjing, China in 2005 and 2010, respectively.

Since 2010, he has been with Nanjing University, Nanjing, China, where he is currently an associate professor with the School of Electronic Science and Engineering. His current research interests include array signal processing and parameter estimation.

JIANGHUI LI received the B.S. degree in communications engineering from Huazhong University of Science and Technology, Wuhan, China in 2011, the M.Sc. degree in communications engineering, and the Ph.D. degree with receiving the K. M. Stott Prize for excellent research in electronics engineering from the University of York, U.K., in 2013 and 2017, respectively. He has been the first researcher receiving the IEEE OES scholarship in U.K.

From 2011 to 2012, he served as a Research Assistant with the Chinese Academy of Sciences, Beijing, China. Since 2017, he has been a Research Fellow with the University of Southampton, U.K. His current research interests include adaptive signal processing, wireless communications, underwater acoustics, and ocean engineering.

YU WU received the B.S. degree in electronic science and engineering from Nanjing University, Nanjing, China, in June 2018. She is currently pursuing the M.S. degree in electrical engineering at California Institute of Technology, CA, USA.

Her research interests include inverse problems in image processing, sparse signal representation, and parameter estimation.

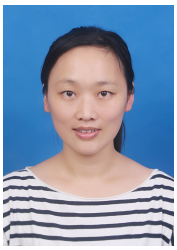

QIONG WANG received the B.S. and the Ph.D. degrees in electronic science and engineering from PLA University of Science and Technology, China, in 2004 and 2011, respectively.

Since 2014, she has been a lecturer at Nanjing University, China. Her current research interests include target automatic recognition and radar target detection.

XINGGAN ZHANG received the B.S. degree in electrical engineering from Nanjing University of Aeronautics and Astronautics, Nanjing, China, in 1982, and the S.M. and Ph.D. degrees from the same University in 1988 and 2001, respectively.

In 1992, he joined the Department of Electronic Engineering at the NUAA, where he was an associate professor. In 1999, he joined the Department of Electronic Science and Engineering at Nanjing University, where he is currently a professor. His research interests include target recognition and image processing.